Check for updates

Controlling the optical properties of chiral nematic mesoporous organosilica films with bioadditives†

Joanna K. Szymkowiak, [ID] [a] Lucas J. Andrew, [ID] [a] Wadood Y. Hamad‡[b] and Mark J. MacLachlan [ID] *[a,c,d]

Chiral nematic mesoporous organosilica (CNMO) films have unique iridescent properties that make them attractive candidates for decorations, sensing and photonics. However, it has proven difficult to control the colour and porosity of CNMO films. Here, we have explored the addition of a range of biodegradable and eco-friendly additives to tune the helical pitch and, hence, the colour of the CNMO materials. It was found that the controlled integration of additives allows for the colour of the materials to be tuned across the visible spectrum, but cannot be used to tune the porosity of the films. This work opens up new prospects for preparation of CNMO materials with adjustable optical properties.

Introduction

Cellulose nanocrystals (CNCs) are a renewable material that can be prepared from the treatment of biomass (*e.g.* wood pulp) with sulfuric acid.[1] These CNCs are typically 5–20 nm in diameter and 100–500 nm in length, depending on the cellulose source and the processing conditions.[2] CNCs are attracting great interest for diverse applications that include reinforcement of polymers, tissue scaffolding, environmental remediation, energy storage, photonic materials, and rheology modifiers.[3–14]

One of the remarkable properties of CNCs is their ability to form a chiral nematic (cholesteric) liquid crystalline phase with a left-handed helical structure above a critical concentration in water.[2] Dried films of CNCs cast from these suspensions retain the chiral nematic structure, wherein the CNCs are effectively organized into layers whose orientation rotates through the film. The repeating distance of the helical organization is called the pitch. When the pitch of the chiral nematic structure in the films matches the wavelength of incident light, it is reflected from the structure. More accurately, the wavelength reflected (λ_{max}) is related to the pitch (P), the refrac-

tive index of the material (n_{avg}), and the angle from the normal of the film (Θ) according to the following equation:[15]

$$\lambda_{max} = n_{avg} \cdot P \cdot \cos(\Theta)$$

Since the optical properties of CNC films were first reported by Gray and co-workers in the 1990s,[16] they have been extensively studied and explored for applications in photonics and sensing.[17–19] For example, Liu and co-workers designed structurally-colored CNC composites doped with glycerol that can be used as iridescent coatings and photonic bio-inks.[20] Yang *et al.* investigated CNC-based materials for optical encryption,[21] paving the way for using anisotropic nanostructures for photonic functional materials including optical coding. The interference colors can be adjusted by varying the angles of rotation between the individual CNC composite film layers from which the multi-layer material is composed, as well as varying the thicknesses and concentrations of CNC components. Recently, the self-assembly of CNC suspensions into photonic films using a coating technique was developed by Vignolini and co-workers.[22] Their methodology is suitable for the large-scale fabrication of structurally colored CNC materials.

The chiral nematic structure of CNCs can be captured in a silica matrix by hydrolyzing and condensing $Si(OMe)_4$ or $Si(OEt)_4$ during the drying of CNCs.[23–25] After removing the CNC template *via* pyrolysis, free-standing chiral nematic mesoporous silica (CNMS) films can be obtained. The materials retain the chiral nematic organization of the CNC template, and therefore also appear iridescent. This concept was further adapted using organosilica precursors with CNC suspensions to afford CNC-organosilica composites; removal of the CNC template from this material by acid hydrolysis resulted in free-standing chiral nematic mesoporous organosilica (CNMO)

[a]Department of Chemistry, University of British Columbia, 2036 Main Mall, Vancouver, British Columbia, V6T 1Z1, Canada. E-mail: mmaclach@chem.ubc.ca
[b]Transformation and Interfaces Group, Bioproducts, FPInnovations, 2665 East Mall, Vancouver, British Columbia, V6T 1Z4, Canada
[c]Stewart Blusson Quantum Matter Institute, University of British Columbia, 2355 East Mall, Vancouver, British Columbia, V6T 1Z4, Canada
[d]WPI Nano Life Science Institute, Kanazawa University, Kanazawa, 920-1192, Japan
†Electronic supplementary information (ESI) available. See DOI: https://doi.org/10.1039/d4nr03326d
‡Current address: Seprify AG, Route de l'Ancienne Papeterie 180, 1723 Marly, Switzerland.

films.[26] Replacing silica with organosilica can improve the flexibility of the materials, and opens up opportunities to tune the material properties by varying the organic group. For example, changing the alkylene spacers in silica precursors resulted in CNMOs with different optical properties and porosity.[27] On the other hand, Terpstra *et al.* prepared CNMO materials *via* a post-synthetic modification route. Incorporating a spiropyran compound into a CNMO film prefunctionalized with amine groups yielded CNMOs with photoswitching and tunable photopatterning properties.[28] Furthermore, we recently reported the two-step modification of CNMOs to introduce hydrophilic and hydrophobic groups *via* thiol–ene click chemistry without disrupting their 'natural' structure.[29]

It is very attractive to be able to tune the reflection wavelength of CNMOs through the controlled addition of suitable additives. Gray *et al.* showed that glucose addition to CNCs led to films with red-shifted reflections.[30] A similar effect was described by Gu *et al.* for CNCs and poly(ethylene glycol) (PEG) composites.[31] In their work, the reflection wavelength of CNC films could be tuned by introducing PEG with varied loadings. With increasing content of PEG up to 30 wt%, the reflection band of the film showed a gradual red-shift. Kelly *et al.* prepared CNMS films with tunable optical properties by adding glucose to CNC-silica composites.[32] The materials obtained were more flexible and less prone to cracking than films prepared without glucose, allowing the researchers to make large, crack-free CNMS films. Varying the glucose content in the composites resulted in CNMS films with tunable reflection wavelengths. However, this concept has previously not been extended to CNMOs; further development in this area of research offers an attractive approach to simultaneously tune the optical properties and improve the processing of CNMO films.

With this in mind, we report here the modification of CNMOs *via* incorporation of various additives (glucose, sucrose, starch, and poly(ethyleneglycol) (PEG-400 and PEG-20 000)) to form composites. This approach allowed us to tune the reflection wavelength of the CNMO films.

Results and discussion

The preparation of CNMO with ethylene spacers (**Et-CNMO**) was carried out using a published procedure,[26] as shown in Fig. 1a.

Organosilica precursor (1,2-bis(trimethoxysilyl)ethane, BTMSE), an aqueous suspension of CNCs (3.25 wt%), and an additive (**2**: glucose, **3**: sucrose, **4**: starch, **5**: PEG-400, **6**: PEG-20 000) were combined in different proportions (0.5–2.5 wt%, Table 1), mixed at room temperature for 20 h, then transferred into a polystyrene Petri dish and left to dry under ambient conditions to afford the desired composite material as a thin film (Fig. S2†). We chose the range up to 2.5 wt% of additives (keeping the CNC concentration at 3.25 wt%) since above this proportion, we observed inhomogeneous composites.
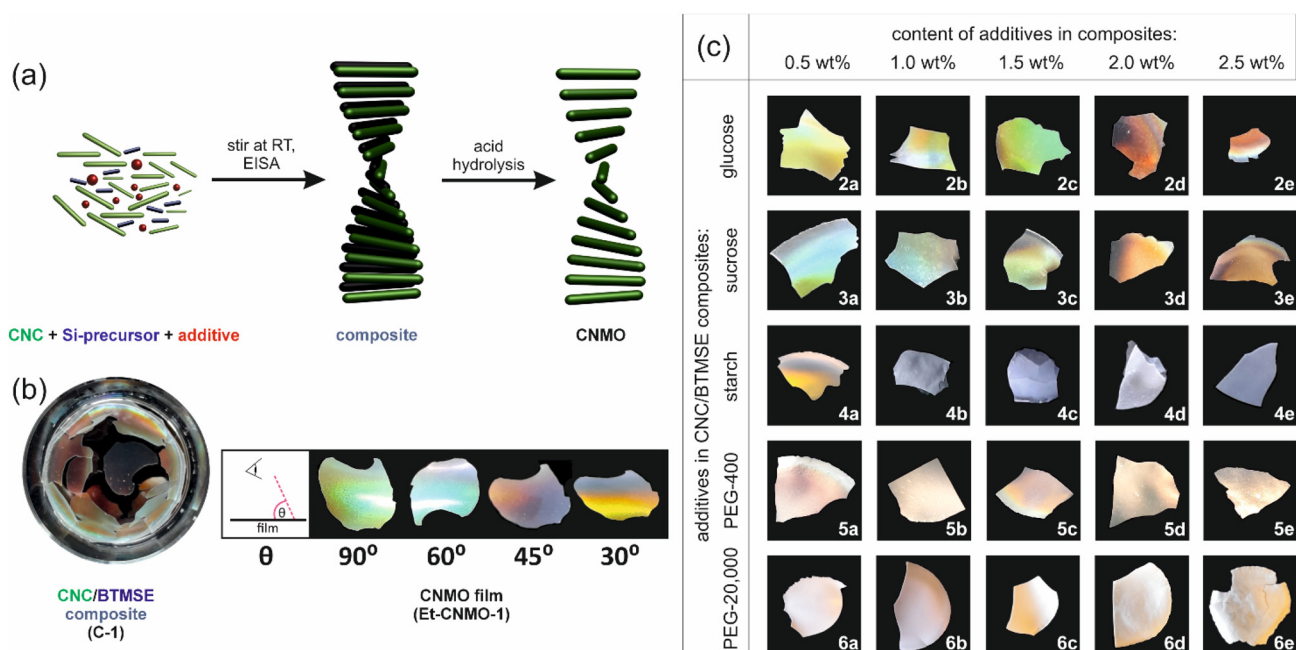

Fig. 1 (a) Preparation of composites and CNMO films. EISA = evaporation-induced self-assembly. (b) Photographs of composites prepared from suspension of CNCs and BTMSE (**C-1**) and product of hydrolysis – organosilica film (**Et-CNMO-1**). The photographs are taken at different angles of film position, and ordered by decreasing viewing angle (*Θ*). (c) Photographs of films of **Et-CNMO-2** to **Et-CNMO-6** prepared from various composites.

Table 1 Composites and CNMO films prepared with CNCs, BTMSE, and additives (glucose, sucrose, starch, PEG-400, PEG-20 000)

Composite	Additive (wt%)		Et-CNMO film
C-1	—	—	**Et-CNMO-1**
C-2a	Glucose	0.5	**Et-CNMO-2a**
C-2b	Glucose	1.0	**Et-CNMO-2b**
C-2c	Glucose	1.5	**Et-CNMO-2c**
C-2d	Glucose	2.0	**Et-CNMO-2d**
C-2e	Glucose	2.5	**Et-CNMO-2e**
C-3a	Sucrose	0.5	**Et-CNMO-3a**
C-3b	Sucrose	1.0	**Et-CNMO-3b**
C-3c	Sucrose	1.5	**Et-CNMO-3c**
C-3d	Sucrose	2.0	**Et-CNMO-3d**
C-3e	Sucrose	2.5	**Et-CNMO-3e**
C-4a	Starch	0.5	**Et-CNMO-4a**
C-4b	Starch	1.0	**Et-CNMO-4b**
C-4c	Starch	1.5	**Et-CNMO-4c**
C-4d	Starch	2.0	**Et-CNMO-4d**
C-4e	Starch	2.5	**Et-CNMO-4e**
C-5a	PEG-400	0.5	**Et-CNMO-5a**
C-5b	PEG-400	1.0	**Et-CNMO-5b**
C-5c	PEG-400	1.5	**Et-CNMO-5c**
C-5d	PEG-400	2.0	**Et-CNMO-5d**
C-5e	PEG-400	2.5	**Et-CNMO-5e**
C-6a	PEG-20 000	0.5	**Et-CNMO-6a**
C-6b	PEG-20 000	1.0	**Et-CNMO-6b**
C-6c	PEG-20 000	1.5	**Et-CNMO-6c**
C-6d	PEG-20 000	2.0	**Et-CNMO-6d**
C-6e	PEG-20 000	2.5	**Et-CNMO-6e**

The composite film prepared from organosilica and CNCs without additive (**C-1**) was iridescent, but brittle. Composite films prepared with 0.5–1.5 wt% content of glucose and sucrose (**C-2a–C-2c** and **C-3a–C-3c**) were slightly iridescent, but still cracked. Those prepared with higher content of sugars (**C-2d,e** and **C-3d,e**) were crack-free and colorless. All composites with starch (**C-3**) were colorless and brittle. Finally, all composites with PEG (**C-5** and **C-6**) were slightly iridescent and crack-free.

The CNC template and carbohydrate additive were removed from the composites by acid hydrolysis according to a published procedure.[26] Then, the organosilica film was dried under ambient conditions for 24 h. As a reference material, the basic **Et-CNMO-1** film was prepared from **C-1**, itself prepared using only CNCs and the organosilica precursor, BTMSE (no additives). Table 1 summarizes the composition of all composites and CNMO films. Photographs of prepared organosilica films are presented in Fig. 1b and c. Materials prepared from composites containing glucose and sucrose were all iridescent and exhibited viewing angle-dependent color as shown in Fig. 1b, but were also brittle. Films prepared with starch (**Et-CNMO-3b–3e**) have a layered structure and are qualitatively more brittle than **Et-CNMO-1**. All materials prepared with PEG appeared white, slightly opalescent, but also brittle. Although it was not possible to obtain crack-free freestanding CNMO films, we were most interested in the effects of the additives to tune the optical properties and perhaps the porosity of the film. FT-IR spectra of **Et-CNMO-1** and CNMO samples prepared using various additives displayed similar patterns (Fig. 2 and Fig. S3–S7†). In particular, the IR spectra

Fig. 2 (a) Selected IR spectra measured for reference **Et-CNMO-1** (black line), and films prepared from various composites: **Et-CNMO-2e** (red line), **Et-CNMO-3e** (green line), **Et-CNMO-4e** (yellow line), **Et-CNMO-5e** (blue line), **Et-CNMO-6e** (pink line). (b) Expanded view of the IR spectra over the range of 1800–650 cm^{-1}. Arrows indicate characteristic bands: 3400 cm^{-1} (O–H stretch); 2892 cm^{-1} (C–H stretch); 1634 cm^{-1} (water bending); 1412 cm^{-1} (C–H bending); 1270 cm^{-1} (C–C stretch); 1157 cm^{-1}, 1096 cm^{-1} and 1015 cm^{-1} (Si–O–Si stretch); 894 cm^{-1} (Si–OH bending); 766 cm^{-1} and 692 cm^{-1} (Si–C stretch).

show several characteristic bands at: 3400 cm^{-1} (O–H stretch); 2892 cm^{-1} (C–H stretch); 1634 cm^{-1} (water bending); 1412 cm^{-1} (C–H bending); 1270 cm^{-1} (C–C stretch); 1157 cm^{-1}, 1096 cm^{-1} and 1015 cm^{-1} (Si–O–Si stretch); 894 cm^{-1} (Si–OH bending); 766 cm^{-1} and 692 cm^{-1} (Si–C stretch).[27,33,34] These data confirm that the compositions are all organosilica, and that the CNCs and additives were removed during the hydrolysis procedure.

Elemental analysis (EA) results of select organosilica films (**Et-CNMO-1**, **Et-CNMO-2e**, **Et-CNMO-3e**, **Et-CNMO-4e**, **Et-CNMO-5e**, and **Et-CNMO-6e**) are shown in Table S1.† Carbon and hydrogen contents in reference organosilica film **Et-CNMO-1** are 13.42% and 3.42%, respectively. Data collected for **Et-CNMO-2e–6e** samples show a slightly lower carbon content and a slightly higher hydrogen content, which are within the ranges 10.37–12.70% and 3.76–4.60%, respectively.

This variation likely results from the presence of different amounts of adsorbed water rather than residual template or additive remaining in the material, which would instead increase the relative carbon content of the samples.

CNMOs have a left-handed chiral nematic structure that originates from the left-handed chiral nematic organization of the CNCs that are used as a template. This structure leads to a reflection band that may be observed as a peak in the UV-vis spectrum and a peak with positive ellipticity in the CD spectrum.[9,24] The films prepared in this study all showed CD signals with positive ellipticity in the UV-vis range, with peak shifts that depend on specific materials. In principle, the position of the maximum reflection depends on both the refractive index of the material and the helical pitch.[22,35] As the modifications do not destroy the rigid (organo)silica structure, we expect that there is nearly insignificant change to the refractive indices, and the main source of peak shifts is due to a change in the helical pitch.

In measured CD spectra, the wavelength of maximum reflection (as observed at the center of the films and measured perpendicular to the film) for basic organosilica **Et-CNMO-1** was observed at 591 nm (Fig. 3). In the case of materials **Et-CNMO-2a–2e** (prepared with glucose), maxima were observed across the range of 562 to 759 nm. In general, increasing the amount of glucose used in the preparation of the CNMO materials led to bathochromic shifts in the reflection peaks.

A similar effect was observed in the case of materials **Et-CNMO-3a–3e**, which were prepared with sucrose. For these composites, the CD signals are in a narrower range than observed with glucose. The absorption maxima are between 582 and 699 nm, and red shifted with increasing amounts of sucrose used in the preparation of the respective organosilica films.

In the case of films prepared with PEG, the results are similar. CD spectra measured for samples prepared with PEG-400 (**Et-CNMO-5**) showed maxima of absorption that are red-shifted in comparison with basic **Et-CNMO-1** film, and the extent of redshift increases with increasing PEG-400 concentration used in the composites. The positive band for sample **Et-CNMO-5a**, which was prepared with the lowest content of PEG-400, is redshifted by 87 nm in comparison to reference material; for others, the shifts are up to nearly 200 nm. In the case of samples prepared with PEG-20 000, samples **Et-CNMO-6a** and **Et-CNMO-6b** show reflection bands at 713 and 747 nm, respectively. Unfortunately, the other films show no iridescence in the measurement range of the instrument, which does not allow for a detailed interpretation. All measured CD and UV-vis spectra are in Fig. S8–S12 and Table S2 in the ESI,† and the effect of additives is summarized in Fig. 3c. Overall, the nature of the additives and their proportion significantly influence the position of the reflectance wavelength of films, and this is even visible to the naked eye.

It is worth comparing the observed changes with other CNC composites reported in the literature. For CNC-glucose materials, the reflection bands tend to move to longer wavelengths with added glucose.[30] In comparison with pure CNC free-standing films, the reflection band measured for

Fig. 3 Measured CD spectra for (a) **Et-CNMO-1** and **Et-CNMO-2** (prepared with glucose); and (b) **Et-CNMO-1** and **Et-CNMO-3** (prepared with sucrose). (c) Plots of the maxima of positive band's wavelength *vs.* amount of additive for **Et-CNMO-1** (reference sample; black dot), **Et-CNMO-2** (prepared with glucose; red triangles), **Et-CNMO-3** (prepared with sucrose; green squares), **Et-CNMO-5** (prepared with PEG-400; yellow diamonds).

CNC-PEG films can be red-shifted up to 120 nm.[31] In the case of CNMS films prepared from CNCs and glucose, Kelly *et al.* reported reflection band changes from 400 to 800 nm. Moreover, using different enantiomers of glucose (L- or D-glucose) had no change in the ellipticity of the CD spectra for CNMS samples – they always showed a left-handed structure.[32]

To summarize, additives influence the optical properties of chiral nematic mesoporous organosilica materials. Inclusion of additives changes the observed color of the films and the position of the characteristic reflection band, while preserving the left-handed chiral nematic organization of cellulose nanocrystals. To understand the effect of additives on the porosity of the CNMO materials, we analyzed the materials through N_2 gas sorption analysis (sample preparation details are given in the ESI†). Gas sorption isotherms for all films indicated a Type IV isotherm with a hysteresis loop consistent with mesoporous materials with cylindrical and spherical pores (H2).[36,37] The specific surface area of **Et-CNMO-1** is 521 m^2 g^{-1}, and pores are centered around 6 nm, agreeing well with results obtained previously for unmodified CNMO materials.[27] All experimental results are reported in Table S3.† In general, there was substantial variation measured for the pore volumes of the CNMO films prepared from different composites. For example, in the case of materials prepared with glucose, measured BET surface areas varied from 436 m^2 g^{-1} for sample **Et-CNMO-2a** up to 955 m^2 g^{-1} for sample **Et-CNMO-2b**. In the case of materials prepared with sucrose, measured BET surface area ranged from 492 m^2 g^{-1} for sample **Et-CNMO-3a**, up to 868 m^2 g^{-1} for sample **Et-CNMO-3b**. In neither series was there a clear trend of the pore size, surface area, or pore volume that would enable one to identify where the additive was positioned relative to the CNCs.

Polarized optical microscopy (POM) images of chiral nematic materials, like CNC or CNMO films, show birefringent textures, a characteristic of chiral nematic organization (Fig. 4).[8,9] POM images collected for the composites show relatively homogeneous films, but with multiple domains, and with black dots – domains of additive that are not birefringent (Fig. 4b). All of the samples with additives showed similar tex-

tures by POM. All POM images collected for composites and CNMO films are shown in the ESI (Fig. S13 and S14†).

Scanning electron microscopy (SEM) images of select samples are shown in Fig. 5. In regions of the cross-section, there are layers observed, which are known to correspond to half of the helical twist in materials with chiral nematic order.[5] As well, defects are apparent in the films that arise from the liquid crystal templating during relatively rapid evaporation of the water in the drying process.[10] Such defects can be controlled and minimized through manipulation of the drying environment during self-assembly, but this work focused primarily on the effect of additives on the properties of CNMO; strict controls over the drying environment were not implemented. CNMO films prepared with additives (Fig. 5d) had the same structure as the base material prepared without any additives (Fig. 5c).

Free-standing chiral nematic mesoporous organosilica (CNMO) films are obtained by the condensation of organosilica precursor and cellulose nanocrystal template, followed by removal of the template with strong acid. These films are iridescent because the pore structure retains the chiral organization of the CNC template. Preparing composites with additives (glucose, sucrose, starch or PEG) yielded composite films, and the template and additive were both readily removed by acid hydrolysis to generate iridescent organosilica films. The identity and molar ratio of the additive affect CNMO film properties in tandem. The amount of additive is critical to control the reflection wavelength. All additives induced a change in the characteristic reflection bands of the composite materials, with starch and PEG causing comparatively higher shifts compared to glucose and sucrose at the same concentrations. Materials ranged in color from blue to red, with a generally consistent trend of higher additive content leading to a more pronounced red-shift in the maximum reflection band. Clearly, with careful selection of additives it is possible to obtain composite organosilica films with reflection bands spanning almost the entire UV-vis range.

Fig. 4 POM images of composite and CNMO films viewed between crossed polarizers. The samples shown correspond to composites prepared from: (a) organosilica precursor and CNC suspension (**C-1**) and (b) organosilica precursor, CNC suspension and sucrose (**C-3e**); and relevant CNMO films: (c) **Et-CNMO-1** and (d) **Et-CNMO-3e**. Red arrows pointing to the non-birefringent regions. Scale bars are 50 μm.
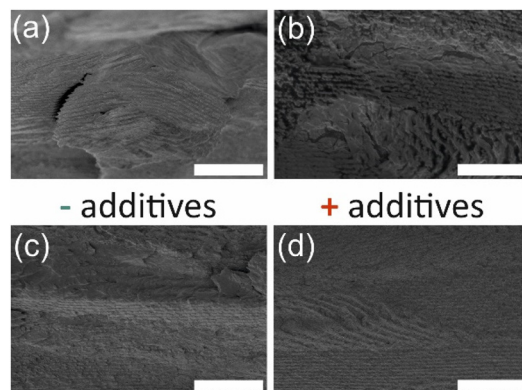

Fig. 5 SEM images (cross section) of composites prepared from: (a) organosilica precursor and CNC suspension (**C-1**) and (b) organosilica precursor, CNC suspension and glucose (**C-2e**); and relevant CNMO films: (c) **Et-CNMO-1** and (d) **Et-CNMO-2e**. Scale bars are 5 μm.

Glucose has been used as a pore-forming agent to prepare porous silica. In this case, hydrogen bonds are formed between D-glucose (used as organic template) and $Si(OR)_{4-x}(OH)_x$ (intermediate silicate species). This interaction brings the two major components together and allows them to form a homogeneous sol without macroscopic silicate particle formation.[38]

In the case of using CNC suspensions and additives, the organization mechanism is more complex than a simple coating of the CNC rods by the additive (as in CNC-glucose/PEG composites),[39,40] or hydrogen-bonded silicate-glucose system (as during mesoporous silica synthesis).[38] Importantly, our experimental data did not show any consistent relationship between the amount of sugar added to the composite and the surface area, pore volume, and pore size of the resulting CNMO material. This suggests that the component organization mechanism is more complex than a simple coating of the CNC rods by the additive. Kelly *et al.* suggested that glucose is mainly integrated into the silica region of the composite, rather than adsorbed to the CNC surface.[32]

Experimental

An aqueous suspension of CNCs was supplied by FPInnovations;[41] and characterized as follows: [CNC] = 3.25 wt%; pH = 3.1; conductivity = (1920 ± 5) μS; zeta potential = (−60 ± 3) mV; average particle size distribution from dynamic light scattering (DLS) = (113 ± 1) nm; length distribution of CNCs = (108 ± 24) nm (calculated from TEM image; number of analyzed nanoparticles: 135); see Fig. S1.† All other reagents were purchased from Sigma Aldrich as reagent grade or higher and used as received. All characterization methods are listed in the ESI.†

In general, organosilica films were prepared by a published two-step procedure with some modification in the first step.[24] In the first step, acid-form CNC suspension (2 mL, 3.25 wt%) was mixed with an additive (**2**: glucose, **3**: sucrose, **4**: starch, **5**: PEG-400, **6**: PEG-20 000) and organosilica precursor (1,2-bis(trimethoxysilyl) ethane, BTMSE, 0.05 mL, 0.2 mmol) to give samples with various additive concentrations (**a**: 0.5, **b**: 1.0, **c**: 1.5, **d**: 2.0, **e**: 2.5 wt%). Mixtures were stirred at room temperature for 20 hours, and then poured into a 25 mm diameter polystyrene Petri dish. Composite films were obtained following evaporation for 3 d under ambient conditions. Organosilica films (CNMO) were obtained from each composite after a hydrolysis step. The reference CNMO film (**Et-CNMO-1**) was prepared with CNC suspension and organosilica precursor following the methodology described above.

To give a specific example, **C-2a** was prepared as follows: aqueous CNC suspension was sonicated for 15 min in an ultrasonic bath and filtered through a syringe filter (PVDF membrane 0.45 μm). Glucose (0.01 g) was dissolved in the CNC suspension (2 mL, 2.02 g, 3.25 wt%), and then BTMSE (0.05 mL, 0.04 g, 0.2 mmol) was added. The mixture was stirred for 20 h at room temperature, and then poured into a 25 mm diameter polystyrene Petri dish. The composite film was isolated following evaporation for 3 d under ambient conditions in the uncovered Petri dish. For the removal of CNCs, the composite film was placed in sulfuric acid (10 mL, 65%) and heated to 100 °C for 18 h. The film was then filtered and washed with a solution of piranha (mixture: H_2O_2 (1 mL 30%) and H_2SO_4 (5 mL 98%)); and water (*ca.* 50 mL) until it appeared colorless. The film was then allowed to air-dry, yielding **CNMO-2a**.

Due to fluctuations in humidity and temperature during drying of the composites, the final base CNMO films show slight differences in reflected wavelength and chiral pitch, which do not affect the further modification methods or the general relationship between properties and structure. Nevertheless, for consistency in the measurements, we used groups of films that were derived from the same batch of CNMO in each set of measurements.

Conclusions

In this work, we explored the use of additives in the preparation of chiral nematic mesoporous organosilicas (CNMOs) in order to tune the optical properties of the materials. The additives could be incorporated without destroying the chiral nematic organization of the materials, leading to iridescent films. By varying the amount of additive, the reflection wavelength of the CNMO films could be tuned across the visible spectrum and into the near-IR. Surprisingly, the porosity of the resulting composite films does not show a clear correlation with addition of additives.

The work provides inspiration for tuning the colors and optical properties of materials using biodegradable and eco-friendly additives that are easy to remove. In addition, the demonstrated relationships between the components of the composites could be the start of research into extending composite materials with additives. The research will also help to expand the library of chiral nematic organosilicas with a variety of optical properties, despite limited availability of organosilica precursors.

Author contributions

J. K. S. designed the project; fabricated the samples; carried out materials characterization, analysis and data visualization; and prepared this manuscript and ESI. L. J. A. carried out N_2 sorption measurements and provided sorption data analysis and assistance with manuscript preparation. W. Y. H. provided a CNC suspension. M. J. M. supervised this work and provided valuable feedback as well as assistance in manuscript preparation.

Data availability

All experimental procedures, characterisation data, supporting spectra, supporting POM images, and other data can be found in the article or in the ESI.†

Conflicts of interest

There are no conflicts to declare.

Acknowledgements

References

1 B. G. Rånby, *Discuss. Faraday Soc.*, 1951, **11**, 158.

2 J.-F. Revol, H. Bradford, J. Giasson, R. H. Marchessault and D. G. Gray, *Int. J. Biol. Macromol.*, 1992, **14**, 170.

3 G. Delepierre, O. M. Vanderfleet, E. Niinivaara, B. Zakani and E. D. Cranston, *Langmuir*, 2021, **37**, 8393.

4 E. S. Ferreira, C. A. Rezende and E. D. Cranston, *Green Chem.*, 2021, **23**, 3542.

5 Y. Habibi, L. A. Lucia and O. J. Rojas, *Chem. Rev.*, 2010, **110**, 3479.

6 R. M. Parker, G. Guidetti, C. A. Williams, T. Zhao, A. Narkevicius, S. Vignolini and B. Frka-Petesic, *Adv. Mater.*, 2018, **30**, 1704477.

7 Z. Wang, C. L. C. Chan, T. H. Zhao, R. M. Parker and S. Vignolini, *Adv. Opt. Mater.*, 2021, **9**, 2100519.

8 M. Giese, L. K. Blusch, M. K. Khan and M. J. MacLachlan, *Angew. Chem., Int. Ed.*, 2015, **54**, 2888.

9 J. A. Kelly, M. Giese, K. E. Shopsowitz, W. Y. Hamad and M. J. MacLachlan, *Acc. Chem. Res.*, 2014, **47**, 1088.

10 A. Tran, C. E. Boott and M. J. MacLachlan, *Adv. Mater.*, 2020, **32**, 1905876.

11 E. C. Emenike, K. O. Iwuozor, O. D. Saliu, J. Ramontja and A. G. Adeniyi, *Carbohydr. Polym. Technol. Appl.*, 2023, **6**, 100337.

12 P. Mali and A. P. Sherje, *Carbohydr. Polym.*, 2022, **275**, 118668.

13 D. Qu, O. J. Rojas, B. Wei and E. Zussman, *Adv. Opt. Mater.*, 2022, **10**, 2201201.

14 P. Lv, X. Lu, L. Wang and W. Feng, *Adv. Funct. Mater.*, 2021, **31**, 2104991.

15 H. De Vries, *Acta Crystallogr.*, 1951, **4**, 219.

16 J.-F. Revol, J. Godbout and D. G. Gray, *J. Pulp Pap. Sci.*, 1998, **24**, 146.

17 P. Grey, S. N. Fernandes, D. Gaspar, E. Fortunato, R. Martins, M. H. Godinho and L. Pereira, *Adv. Funct. Mater.*, 2019, **29**, 1805279.

18 L. Bai, Z. Wang, Y. He, F. Song, X. Wang and Y. Wang, *ACS Sustainable Chem. Eng.*, 2020, **8**, 18484.

19 G. Zhao, Y. Zhang, S. Zhai, J. Sugiyama, M. Pan, J. Shi and H. Lu, *ACS Appl. Mater. Interfaces*, 2020, **12**, 17833.

20 M. Xu, W. Li, C. Ma, H. Yu, Y. Wu, Y. Wang, Z. Chen, J. Li and S. Liu, *J. Mater. Chem. C*, 2018, **6**, 5391.

21 Y. Yang, X. Wang, H. Huang, S. Cui, Y. Chen, X. Wang and K. Zhang, *Adv. Opt. Mater.*, 2020, **8**, 2000547.

22 B. E. Droguet, H.-L. Liang, B. Frka-Petesic, R. M. Parker, M. F. L. De Volder, J. J. Baumberg and S. Vignolini, *Nat. Mater.*, 2022, **21**, 352.

23 K. E. Shopsowitz, H. Qi, W. Y. Hamad and M. J. MacLachlan, *Nature*, 2010, **468**, 422.

24 E. Dujardin, M. Blaseby and S. Mann, *J. Mater. Chem.*, 2003, **13**, 696.

25 C. F. J. Faul and M. Antonietti, *Adv. Mater.*, 2003, **15**, 673.

26 K. E. Shopsowitz, W. Y. Hamad and M. J. MacLachlan, *J. Am. Chem. Soc.*, 2012, **134**, 867.

27 A. S. Terpstra, L. P. Arnett, A. P. Manning, C. A. Michal, W. Y. Hamad and M. J. MacLachlan, *Adv. Opt. Mater.*, 2018, **6**, 1800163.

28 A. S. Terpstra, W. Y. Hamad and M. J. MacLachlan, *Adv. Funct. Mater.*, 2017, **27**, 1703346.

29 J. K. Szymkowiak, C. M. Walters, W. Y. Hamad and M. J. MacLachlan, *Eur. J. Inorg. Chem.*, 2022, **2022**, e202200218.

30 X. Mu and D. G. Gray, *Langmuir*, 2014, **30**, 9256.

31 M. Gu, C. Jiang, D. Liu, N. Prempeh and I. I. Smalyukh, *ACS Appl. Mater. Interfaces*, 2016, **8**, 32565.

32 J. A. Kelly, M. Yu, W. Y. Hamad and M. J. MacLachlan, *Adv. Opt. Mater.*, 2013, **1**, 295.

33 S. R. Darmakkolla, H. Tran, A. Gupta and S. B. Rananavare, *RSC Adv.*, 2016, **6**, 93219.

34 O. Muth, C. Schellbach and M. Fröba, *Chem. Commun.*, 2001, 2032.

35 J. A. Kelly, C. P. K. Manchee, S. Cheng, J. M. Ahn, K. E. Shopsowitz, W. Y. Hamad and M. J. MacLachlan, *J. Mater. Chem. C*, 2014, **2**, 5093.

36 J. Rouquerol, D. Avnir, C. W. Fairbridge, D. H. Everett, J. H. Haynes, N. Pernicone, J. D. F. Ramsay, K. S. W. Sing and K. K. Unger, *Pure Appl. Chem.*, 1994, **66**, 1739.

37 K. S. W. Sing, D. H. Everett, R. A. W. Haul, L. Moscou, R. A. Pierotti, J. Rouquérol and T. Simieniewska, *Pure Appl. Chem.*, 1985, **57**, 603.

38 Y. Wei, J. Xu, H. Dong, J. H. Dong, K. Qiu and S. A. Jansen-Varnum, *Chem. Mater.*, 1999, **11**, 2023.

39 K. Yao, Q. Meng, V. Bulone and Q. Zhou, *Adv. Mater.*, 2017, **29**, 1701323.

40 X. Zou, R. Xue, Z. An, H. Li, J. Zhang, Y. Jiang, L. Huang, W. Wu, S. Wang, G.-H. Hu, R. K. Y. Li and H. Zhao, *Small*, 2024, **20**, 2303778.

41 W. Hamad, *Can. J. Chem. Eng.*, 2006, **84**, 513.